Solving the Schrödinger Equation in Arbitrary Quantum-Well Potential Profiles Using the Transfer Matrix Method

BJÖRN JONSSON AND SVERRE T. ENG, MEMBER, IEEE

Abstract—**We present a simple, accurate, and fast algorithm for solving the one-dimensional time-independent Schrödinger equation. The algorithm is based on the transfer matrix method. We can thus calculate all bound and quasi-bound energy levels and the corresponding wave functions for an arbitrarily shaped potential profile. The results of our calculations are compared with those obtained by other authors for various types of problems. A central part of this paper deals with the solving of the Schrödinger equation in quantum-well structures. Our results show that the transfer matrix method is as accurate as other methods, but it is easier to implement and, hence, is superior for calculations on small computers, such as a PC.**

I. Introduction

In recent years there has been a considerable increase in research activities directed towards the development of optoelectronic devices based on quantum-well structures [1]–[4]. The work and time spent to develop a new device is, however, very high and in order to better understand the physical properties of a device it is important that one can simulate the expected performance on a computer. Scientists working with the processing technique, without expert knowledge in numerical computation, must be able to implement computer models, appropriate to their problem, on their own. Therefore, it is important with simple methods that give useful and accurate results on PC-level computers. Such methods must be both easy to implement and relatively fast. Furthermore, they must be tested on a wide range of structures to ensure that they are well behaved.

In this paper we present a simple, accurate, and fast algorithm for numerically solving the Schrödinger equation in quantum-well structures. The algorithm is based on the transfer matrix method (TMM). The TMM is a general numerical method that can be used for a wide range of problems dealing with second-order differential equations. One example is the calculation of propagation characteristics in planar waveguides, presented by Walpita, [5] and in a modified form by Ghatak *et al.* [6]. One other example of the TMM is given in [7], where the spontaneous emission in a DFB-laser is investigated. The TMM is simple to implement and gives accurate results to three or four digits, which is more than sufficient for most applications. In [8] the TMM with Airy-functions is used to calculate the energy levels of a variably spaced superlattice energy filter (VSSEF). To our knowledge this is, however, the first time the transfer matrix method is extensively compared with various other methods for solving the Schrödinger equation in problems related to quantum-well structures. The practical limits and the usefulness of the TMM are reviewed, and our results are compared with results obtained using several other methods. Furthermore, we examine the importance of including the variation of the effective mass with aluminum concentration into the calculations. This variation is, however, often neglected by other authors.

Various methods have been presented to solve the Schrödinger equation numerically. Two examples are the WKB approximation [9] and the variational calculations [10], [11]. Ghatak *et al.* [12] present a matrix method, for solving the Schrödinger equation in quantum-well structures, which in principle is quite similar to this method. In [13] the energy levels are found by the stabilization method of quantum chemistry. Furthermore, many methods dealing with these problems are cumbersome to implement. Two such examples are the Monte Carlo method [14] and the finite element method (FEM) [15], [16]. To implement algorithms based on these methods expert knowledge in computer science is required. The method described here, the TMM, is simple to implement and gives quick and accurate answers to complex problems.

This paper is outlined as follows: in Section II, we will give a brief explanation of the theory behind the transfer matrix method and its implementation. Section III contains several examples of results obtained with our program and a comparison of these results with those of others. This is done both for single quantum-well (SQW) structures and superlattice structures. In addition, we investigate the problem with SQW structures and superlattices in an applied electric field and take the variation of the effective mass with varying aluminum concentration into account. Finally, in Section IV, we discuss some advantages and disadvantages with the transfer matrix method compared to other methods.

Manuscript received February 16, 1990; revised July 12, 1990. This work was supported by the National Swedish Board for Technical Development (STU).

The authors are with Department of Optoelectronics and Electrical Measurements, Chalmers University of Technology, S-412 96 Göteborg, Sweden.

IEEE Log Number 9039201.

II. Theory

The properties of charged particles in a semiconductor material can be found by solving the Schrödinger equation

$$i\frac{h}{2\pi}\cdot\frac{\partial u(r,t)}{\partial t}=\left[\frac{-h^2}{8\pi^2\cdot m}\cdot\nabla^2+v(r,t)\right]u(r,t) \tag{1}$$

where the variables r and t denote space-coordinate and time-coordinate, respectively. The particle mass is denoted m and h is Planck's constant. Furthermore, the electric potential in which the particle is moving is denoted by $v(r,t)$, which indicates that it can be both time and space dependent. The unknown, space and time-dependent, wave function is denoted by $u(r,t)$.

We follow the envelope-function approximation presented by Bastard [17], [18]. In this approximation all rapidly varying phenomena, on the scale of atomic cells, are discarded and the wave function $u(r,t)$ can be separated in one time-dependent and one time-independent part.

$$u(r,t)=\Psi(r)\cdot e^{-2\pi iEt/h} \tag{2}$$

where $\Psi(r)$ is the steady-state solution, and E is the energy eigenvalue. If we adopt the effective-mass approximation [16]–[18] and only study steady-state problems in one-dimension, (1) can be expressed as

$$\left[\frac{-h^2}{8\pi^2}\frac{d}{dx}\frac{1}{m^*(x)}\frac{d}{dx}+V(x)\right]\Psi(x)=E\Psi(x) \tag{3}$$

where the variation in space of the particle's effective mass is expressed by $m^*(x)$.

In order to discretize the problem, we consider a piecewise constant potential profile, as shown in Fig. 1 where we have a total of N layers, starting with layer No. 0 (for $-\infty < x \le x_0$) to layer No. $N-1$ (for $x > x_{N-2}$). In each of these layers both the potential V_j and the effective mass m_j^* are assumed to have a constant value. Our problem is now to solve (3) in each layer for a given potential profile. Within each layer the wave functions can be expressed as exponential functions according to Euler's formulas and we write for the wave function in layer number j

$$\Psi_j(x)=A_j\cdot e^{p_j(x)}+B_j\cdot e^{-p_j(x)} \tag{4}$$

where $p_j(x)$ is a complex function, given by

$$p_j(x)=\begin{cases}\Gamma_0\cdot x & (j=0)\\ \Gamma_j\cdot(x-x_{j-1}) & (j>0).\end{cases} \tag{5}$$

The unknown complex constants A_j and B_j are to be determined by the boundary conditions for the wave functions. The variable Γ_j is related to the eigenvalue E by the expression

$$\Gamma_j(E)=i\cdot\sqrt{\frac{8\pi^2\cdot m_j^*}{h^2}\cdot(E-V_j)}. \tag{6}$$

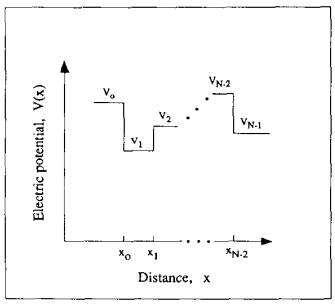

Fig. 1. A piecewise constant potential profile consisting of N layers.

If $E < V_j$ then Γ_j is real and negative, otherwise it is complex. Note that, so far, we have said nothing about the actual shape of the wave function except that within each layer it must be possible to write it as a linear combination of complex exponential functions as in (4).

The boundary conditions for the wave functions at the border between two layers can be written as (according to Fig. 1 the x-coordinate at the boundary between layer j and $j-1$ has the value x_{j-1})

$$\Psi_{j-1}(x_{j-1})=\Psi_j(x_{j-1}) \tag{7}$$

$$\frac{1}{m_{j-1}^*}\cdot\frac{d}{dx}\left[\Psi_{j-1}(x_{j-1})\right]=\frac{1}{m_j^*}\cdot\frac{d}{dx}\left[\Psi_j(x_{j-1})\right]. \tag{8}$$

It was shown by Bastard [17] that for a quantum well the particle current is not conserved, hence, the factor $1/m^*$ in (8). As further pointed out by Bastard, the boundary condition in (8) is the only one which ensures stationary eigenstates even if there is a jump in the effective mass at the boundaries. The total wave function for the system Ψ is now given by summing the wave functions, Ψ_j in all individual layers together. It should be pointed out here that the process of discretizing (3), with piecewise constant effective mass and potential values, implies that the wave functions in (4) are only valid within each layer and not at the very boundary points. However, this does not in any way restrict the generality of the numerical method presented here.

Applying the boundary conditions in (7) and (8) to (4), it is possible to derive an expression that relates the A and B constants in layer $j+1$ to the constants in layer j in the following way:

$$\begin{bmatrix}A_{j+1}\\ B_{j+1}\end{bmatrix}=M_j\cdot\begin{bmatrix}A_j\\ B_j\end{bmatrix} \tag{9}$$

where M_j is a 2×2 matrix. By repeatedly applying (9), we can find a relation between the A and B coefficients in the outermost layers

$$\begin{bmatrix}A_{N-1}\\ B_{N-1}\end{bmatrix}=M_{N-2}\cdot M_{N-1}\cdot\cdots\cdot M_1\cdot M_0\cdot\begin{bmatrix}A_0\\ B_0\end{bmatrix}$$

$$=\begin{bmatrix}\alpha_{11} & \alpha_{12}\\ \alpha_{21} & \alpha_{22}\end{bmatrix}\cdot\begin{bmatrix}A_0\\ B_0\end{bmatrix}. \tag{10}$$

We still need one more constraint to be put on the solution. The wave functions should be bound in space, that is, they should be zero in amplitude when x tends to plus or minus infinity. As can be seen in (4), this constraint demands that $A_0 = 0$ and $B_{N-1} = 0$, which is satisfied if the coefficient α_{22} equals zero in (10). In other words, we have found a solution to (3) whenever we have an eigenvalue E that fulfills the requirement

$$\alpha_{22}(E) = 0. \tag{11}$$

Note that α_{22}, in general, is complex and both the real and imaginary parts should be zero to satisfy the eigenvalue conditions.

By dividing the potential into several layers with a constant potential profile within each layer it is now possible to solve the one-dimensional Schrödinger equation for an arbitrary potential profile. We have implemented an algorithm for solving (11), for an N-layer potential profile. This algorithm is explained in detail in [19]. The problem has been tested on a microcomputer, based on a Motorola 68010 processor. The average time for calculating four energy levels and the corresponding wave functions is about two minutes for a 40-layer potential profile. Usually the time spent for presenting the output to the user (i.e., plotting curves and diagrams) is in the order of several minutes, and therefore we do not see any reason for optimizing the code with respect to speed at this moment.

The wave functions in an arbitrary piecewise linear potential profile, as shown in Fig. 2, can be expressed as a linear combination of Airy-functions [8], [13], [20]–[22]. The wave functions in each layer can thus be solved by using (12), below, instead of (4)

$$\Psi_j(x) = \begin{cases} A_j \cdot Ai(z_j) + B_j \cdot Bi(z_j) & 1 \le j \le N-2 \\ A_j \cdot e^{p_j(x)} & j = 0 \text{ or } N-1 \end{cases} \tag{12}$$

where $Ai(x)$ and $Bi(x)$ are Airy-functions; z_j is defined in [22]; and p_j in (8). The energy values and wave functions can now be solved from (12) in exactly the same way as described above.

For calculations concerning $Al_xGa_{1-x}As$ material we have used the formulas given by Adachi in [23] to calculate the effective mass and potential profile. If an external electric field is applied, the potential profile will be changed according to the equation

$$V(x, \mathcal{F}) = V(x, 0) - e \cdot x \cdot \mathcal{F} \tag{13}$$

where $\mathcal{F}$ is an applied external electric field, in V/m, and $V(x, 0)$ is the potential profile without any applied field. The elementary charge is denoted by e and x is the space coordinate.

III. Numerical Examples

We have investigated the usefulness and limitations of the transfer matrix method by comparing our results with those obtained by other authors for a number of different problems concerning quantum-well applications in AlGaAs material. In this section, we give a number of examples and for each example we have compared our results with those of others. In the first part of this paragraph we have calculated the energy levels in SQW structures in $Al_xGa_{1-x}As$ material, without any external electric field. We then continue by investigating the effect of an applied external uniform electric field and finally we examine the location of the energy levels in a VSSEF structure. For convenience parameters used for the calculations of all described structures are given in Table I.

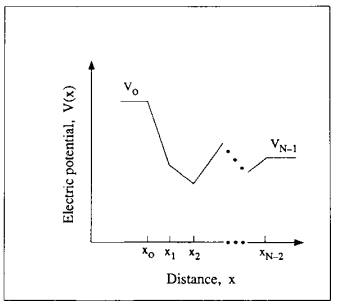

Fig. 2. An arbitrary piecewise linear potential profile consisting of N layers.

A. A Rectangular Quantum Well in $Al_xGa_{1-x}As$ Material

We first consider an SQW with parameters according to column A in Table I. As stated in [23], the effective masses of electrons and holes vary with the concentration of aluminum and should therefore have a different value inside the well than outside the well. We show results obtained both with a varying effective mass approximation (VEM) and by setting the effective mass to a constant value throughout the structure (CEM). In Table II, we compare our results obtained with the TMM, with those of Nakamura *et al.* [16], who have used a FEM program. According to the formulas in [23] a percentage of aluminum of $x = 30\%$ would give a well depth of $V_e = 224.4$ meV. Since [16] obviously has made calculations on the case $V_e = 225.0$ meV we present our results for this case too. As can be seen in Table II, there is an excellent agreement for the VEM case between our results and those of the more complex FEM analysis performed by Nakamura *et al.* However, there is a substantial difference between the CEM results and those obtained with the VEM approximation. Thus, the variation of the effective mass in the structure can not be neglected if one desires accurate results.

Bajema *et al.* [24], have experimentally investigated the intersubband transition of photoexcited electrons in SQW structures by Raman spectroscopy. The parameters for their structure are given in columns B and C in Table I. For such wide quantum wells as in this example ($L = 264$ Å), the energy levels will be located very close to each other. We have calculated the location of the two lowest energy levels in the quantum well. These calculations have

TABLE I
PARAMETERS USED FOR THE CALCULATIONS. THE EFFECTIVE MASS VALUES ARE EXPRESSED IN UNITS OF THE ELECTRON REST MASS, m_0.

		A	B	C	D	E	F	G	H
Percentage of Al, x		30 %	30 %	30 %	38 %	–	41.58 %	54 %	45 %
Band splitting offset, Q_c		60 %	60 %	60 %	85 %	–	60 %	85 %	85 %
Well width, L [Å]		200	264	264	30	50	300	37	[a]
Well depth for electrons, V_e [meV]		224	224	317	400	10^6	311	–	477
Well depth for holes, V_h [meV]		149	149	56	71	–	–	103	–
Effective mass, CEM									
Electrons		0.067	–	–	0.067	1.0	0.067	–	–
Heavy holes		0.45	–	–	0.45	–	–	0.45	–
Light holes		0.10	–	–	0.085	–	–	–	–
Effective mass, VEM									
Electrons	inside well	0.067	0.067	0.067	0.067	–	0.067	–	0.067
	outside well	0.0919	0.0919	0.0919	0.0985	–	0.1015	–	0.1043
Heavy holes	inside well	0.51	–	–	0.51	–	–	0.51	–
	outside well	0.582	–	–	0.601	–	–	0.601	–
Light holes	inside well	0.085	–	–	0.085	–	–	–	–
	outside well	0.104	–	–	0.109	–	–	–	–
Results compared to ref.		[16]	[24]	[24]	[12]	[25]	[16]	[21]	[8]

[a]Calculations made on a VSSEF structure. See Fig. 6 for details.

TABLE II
CALCULATED VALUES FOR THE FOUR LOWEST ENERGY LEVELS FOR ELECTRONS (El), HEAVY HOLES (Hh), AND LIGHT HOLES (Lh) IN THE SQW STRUCTURE IN COLUMN A IN TABLE I. THE TMM RESULTS ARE COMPARED WITH THOSE OF [16] WHO USED A FEM PROGRAM.

		Energy levels [meV]			
Level No		This work (TMM)		[16] (FEM)	
		CEM	VEM	VEM	VEM
		V_e = 224.4 [meV]		V_e = 225.0 [meV]	
El	1	10.42	9.962	9.966	9.967
	2	41.38	39.75	39.77	39.77
	3	91.82	88.88	88.92	88.93
	4	158.76	155.51	155.59	155.61
		V_h = 71 [meV]			
Hh	1	1.81	1.59	–	–
	2	7.22	6.37	–	–
	3	16.22	14.32	–	–
	4	28.77	25.42	–	–
Lh	1	6.98	7.78	–	–
	2	27.71	30.95	–	–
	3	61.47	68.78	–	–
	4	106.3	118.67	–	–

been made for two different values of the band-splitting parameter Q_c. The results in Table III show that we have bracketed the experimental value of the energy difference ΔE obtained by Bajema *et al.* Thus, the importance of knowing a correct value of the band-splitting parameter Q_c cannot be emphasized enough. Our calculation indicates that, in this example, a value of $Q_c \approx 70\%$ would correspond to the experimental results.

TABLE III
LOCATION OF THE TWO LOWEST ENERGY LEVELS IN THE STRUCTURES DESCRIBED IN COLUMNS B AND C IN TABLE I. THE ENERGY LEVELS ARE CALCULATED FOR ELECTRONS WITH THE TMM PROGRAM FOR TWO DIFFERENT VALUES OF THE BAND-SPLITTING PARAMETER Q_c. THE ENERGY DIFFERENCE BETWEEN LEVELS E_1 AND E_2 HAS BEEN MEASURED BY BAJEMA *et al.* [24]. ENERGY VALUES ARE IN meV.

	This work, TMM		[24]
	Q_c = 60%	Q_c = 85%	
Ground state level, E_1	6.18	6.43	–
Second state level, E_2	24.70	25.72	–
Energy difference, ΔE	18.52	19.29	18.9

B. An SQW with an Applied Field

In Fig. 3 we show the potential profile and ground state wave function for an electric field of 100 and 400 kV/cm, applied to the SQW structure in column D in Table I. These parameters correspond to an $Al_xGa_{1-x}As$ material with 38% aluminum ($x = 0.38$) and a band-splitting ratio of 85:15 ($Q_c = 0.85$). Note that a band-splitting offset of 85:15 would result in a well depth of $V_e = 402$ meV according to [23], but in order to compare our calculations with those of Ghatak *et al.* we use the value $V_e = 400$ meV in this example. We have used a 24-layer approximation to describe the quantum well and the region outside the well. The potential is assumed to be constant from minus infinity to $x = 0$ and from $x = 170$ Å to plus infinity, as shown in Fig. 3. The parameters of this SQW are chosen in such a way that only one bound energy level exists. In this example we have tested the TMM algorithm with both a sine–cosine wave function approximation according to (4) and an Airy-function approximation according to (12). In Table IV, we compare our calculated results with those of Ghatak *et al.* (see [12]). It is seen that there is an excellent agreement between our results and those of Ghatak *et al.* However, if the variation of the effective mass is taken into account, the location of the energy levels are substantially shifted. The difference between 178.3 meV for a constant effective mass approximation and 158.9 meV for a variable effective mass calculation is indeed important. Comparing this result and those in Table II, the conclusion is that if we want to make accurate calculations of the location of the bound energy levels in AlGaAs material, it is far more important to take the variation of the effective mass into account than to use the most sophisticated numerical algorithm.

In Appendix B of [25], Miller *et al.* describe an "exact solution for a particle in an infinite well in the presence of a uniform static field". It would be interesting to compare their analytical solution with this numerical method. We have therefore made calculations on the same type of problem. The results in [24] are presented as normalized ground state energy versus normalized electric field, but this can easily be converted into common units of eV and V/m, according to the following relations. (E_n is the nth energy level and F is the applied field.)

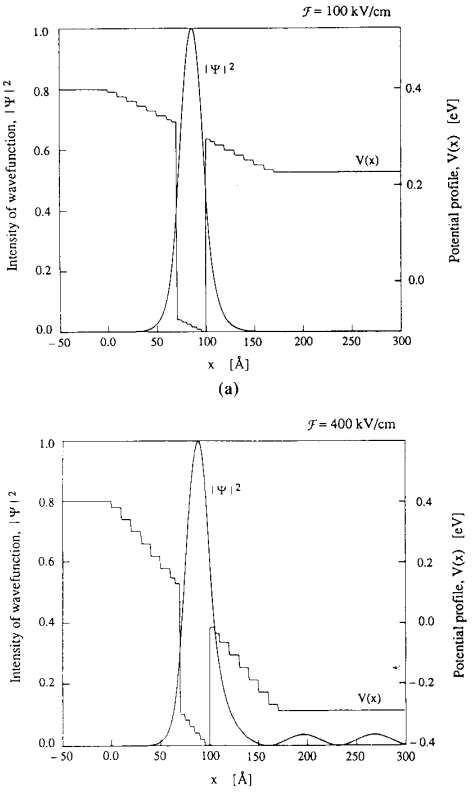

Fig. 3. The intensity of the wave function for the ground state energy level in the 30 Å SQW structure described in column D of Table I. a) $\mathcal{F}$ = 100 kV/cm b) $\mathcal{F}$ = 400 kV/cm.

$$E_{\text{norm}} = \frac{E_n}{W_1} \tag{14}$$

$$F_{\text{norm}} = \frac{e \cdot L \cdot F}{W_1} \tag{15}$$

where

$$W_1 = \frac{h^2}{8 \cdot m^* \cdot L^2}. \tag{16}$$

TABLE IV
CALCULATED ENERGY LEVELS FOR AN SQW POTENTIAL PROFILE WITH AN APPLIED ELECTRIC FIELD. WE COMPARE RESULTS CALCULATED WITH THE SINE-COSINE WAVE FUNCTIONS ACCORDING TO (4) (SINE-COSINE); AIRY-FUNCTION WAVE FUNCTIONS ACCORDING TO (12) (AIRY-FUNCTION); AND GHATAK *et al.* [12]. PARAMETERS USED FOR THE CALCULATIONS ARE GIVEN IN COLUMN D IN TABLE I.

Applied field [kV/cm]		Energy levels [meV]			
		Sine-cosine		Airy-function	[12]
		VEM	CEM	CEM	CEM
Electrons	0	158.9	178.3	–	178.3
	100	158.4	177.6	177.6	177.4
	200	157.0	175.5	175.7	175.7
	300	154.4	171.9	172.1	172.3
	400	151.1	167.0	–	167.1
Heavy holes	0	25.9	29.0	–	–
	100	23.0	25.0	–	–
	200	21.1	18.7	–	–
Light holes	0	51.0	53.5	–	–

For our calculations we used the parameters in column E of Table I. The well is divided into ten layers of 5 Å each and the well depth is set to 1 keV, which approximately gives an infinitely deep well. The effective masses are set to a constant value of $1.0 \cdot m_0$ throughout the structure. In Fig. 4 we compare our results for the ground state energy level with those of Miller *et al.* [25]. As can be seen the TMM results correspond precisely to the analytical solution and is clearly better than the variational solution.

Nakamura *et al.* [16] have calculated the energy shift due to an electric field for the three lowest energy levels in the SQW structure given in column F of Table I. In [16] a FEM program was used and the result was plotted in a diagram with normalized energy levels versus normalized field, according to (14) and (15) above. In Table V, we show our results obtained with the TMM algorithm and the FEM results read from diagrams in [16]. For the TMM calculations the structure was divided into 40 layers (30 layers of 10 Å each inside the SQW and 5 layers of 20 Å on each side). We see that the TMM give just as accurate results as the more complex FEM program. Comparing the CEM and VEM columns we see that the energy levels for constant effective mass are located higher up in the quantum well than those calculated with a variable effective mass, as expected. Once again we show the importance of taking the variation of the effective mass into consideration.

When a strong electric field is applied to an SQW structure the system may not have true bound states. The particles, initially confined in a well, can lower their potential energy by tunneling out of the well. However, it may be that the tunneling probability is small and in such a case the system has quasi-bound states. The carriers are thus captured inside the potential well for a considerable

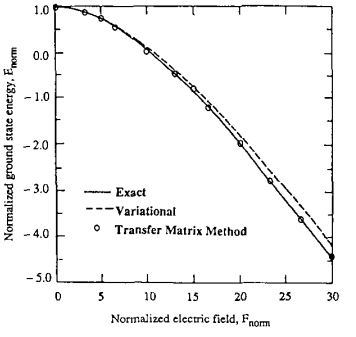

Fig. 4. The change in the ground-state energy level as a function of an applied electric field for an infinitely deep SQW. The "exact" and "variational" results, shown as a solid and dotted lines are taken from Miller *et al.* [25]. The results, calculated by the transfer matrix method are marked with circles. The E_{norm} and F_{norm} values are calculated according to (14) and (15).

period of time before they tunnel out. In the case of quasi-bound states, the eigenvalues (energy levels) may be complex. Following the notation used by Ahn and Chuang [21], we define a complex eigenvalue

$$E = E_{re} - i \cdot E_{im} \tag{17}$$

where E_{im} is found to be positive. The parameter E_{im} can be related to the tunneling probability per unit time, which in turn is a measure of the lifetime of the quasi-bound particles. Calculations of quasi-bound states in SQW structures have been made in [12] and [21]. By substituting (17) into (2) we may directly obtain the total time and space-dependent wave function

$$u(x, t) = \Psi(x) \cdot e^{-2\pi i \cdot E_{re} \cdot t/h} \cdot e^{-2\pi \cdot E_{im} \cdot t/h}. \tag{18}$$

Thus, the lifetime τ associated with the particle is given

TABLE V
CALCULATED NORMALIZED ENERGY LEVELS FOR ELECTRONS IN AN SQW STRUCTURE DESCRIBED IN COLUMN F OF TABLE I. THE NORMALIZED ELECTRIC FIELD AND ENERGY LEVELS ARE CALCULATED ACCORDING TO (14) AND (15). RESULTS OBTAINED WITH THE TMM PROGRAM ARE COMPARED TO THOSE OF NAKAMURA *et al.* [16], WHO USED A FEM PROGRAM. ENERGY LEVELS ARE NORMALIZED TO THE VALUE $W_1 = 6.236$ meV.

Applied field			Normalized energy levels		
F_{norm}	F [kV/cm]	Energy level	This work, TMM		[16], FEM
			CEM	VEM	VEM
0	0.0	E_1	0.84	0.81	0.8
		E_2	3.36	3.24	3.3
		E_3	7.54	7.29	7.3
20	41.57	E_1	− 2.89	− 3.07	− 3.1
		E_2	3.10	2.94	3.1
		E_3	8.24	8.04	8.1
40	83.14	E_1	− 9.15	− 9.48	− 9.4
		E_2	0.30	− 0.03	0.1
		E_3	8.02	7.81	7.8
60	124.7	E_1	− 16.18	− 16.68	− 16.7
		E_2	− 3.88	− 4.25	− 4.1
		E_3	6.04	5.82	–
80	166.3	E_1	− 23.7	− 24.3	− 24.3
		E_2	− 8.98	− 9.36	–
		E_3	2.66	2.49	–

TABLE VI
QUASI-BOUND COMPLEX GROUND ENERGY LEVELS FOR HEAVY HOLES IN AN SQW WITH AN APPLIED ELECTRIC FIELD. THE TMM IS COMPARED WITH THE RESONANCE METHOD; THE PHASE-SHIFT METHOD; AND THE STABILIZATION METHOD DESCRIBED IN [21]. PARAMETERS USED ARE GIVEN IN COLUMN G IN TABLE I. THE ENERGY LEVEL E IS EXPRESSED AS A COMPLEX NUMBER; $E = E_{re} - I \cdot E_{im}$. THE LIFETIME τ HAS BEEN CALCULATED FROM E_{im} ACCORDING TO (19).

Applied field			Energy levels and lifetimes				
[kV/cm]			TMM		Resonance	Phase-Shift	Stabilization
			VEM	CEM	CEM	CEM	CEM
0	E_{re}	[meV]	23.0	26.3	–	–	–
	E_{im}	[μeV]	0.00	0.00	–	–	–
75	E_{re}	[meV]	21.9	25.2	25.17	25.17	25.17
	E_{im}	[μeV]	0.46	1.1	0.93	0.95	4.3
	τ	[ps]	1.4	0.60	0.71	0.69	0.15
100	E_{re}	[meV]	21.1	24.2	24.21	24.21	24.21
	E_{im}	[μeV]	1.58	21.5	18	18	20
	τ	[ps]	0.42	0.031	0.037	0.037	0.033
150	E_{re}	[meV]	18.1	21.5	21.37	21.38	21.17
	E_{im}	[μeV]	64.3	143	320	320	325
	τ	[ps]	0.010	0.0046	0.0021	0.0021	0.0020

TABLE VII
CALCULATED LIFETIMES τ FOR ELECTRONS IN AN SQW WITH AN APPLIED ELECTRIC FIELD. THE TMM IS COMPARED WITH THE METHOD DESCRIBED IN [12]. PARAMETERS USED ARE GIVEN IN COLUMN D IN TABLE I.

Applied field	Lifetime [ps]	
[kV/cm]	TMM, CEM	[12]
0	∞	∞
100	∞	180000
150	658	170
200	41	9
250	4.6	0.5
300	1.3	0.3
350	3.6	0.1

by the relation

$$\tau = \frac{h}{2\pi \cdot E_{\text{im}}}. \tag{19}$$

The location of the energy levels for heavy holes in a 37 Å wide SQW with 100 meV high walls, submitted to an electric field are calculated in [21]. For this narrow well there exists only one energy level. The parameters used for the calculations are shown in column G of Table I. Our results were obtained with the TMM program by dividing the structure into 29 layers. It is readily seen in Table VI that the results calculated with the TMM agree well with the phase-shift analysis, the stabilization method, and the resonance method described in [21]. Returning to the SQW structure in column D in Table I, we have also used the TMM with constant effective masses and a 24-layer approximation of the potential profile to calculate the lifetimes for the quasi-bound states. In Table VII, these calculated lifetimes are compared with those predicted in [12]. As can be seen by comparing the results in Table VI and VII there is a great uncertainty in the calculated values of E_{im} and τ. This difference is, however, small compared to the change in the location of the energy levels that are imposed by applying the variable effective mass approximation.

C. A VSSEF Structure

Finally, we will calculate the location of energy levels in the VSSEF structure presented in column H of Table I and Fig. 5. Our results are compared to those obtained by Brennan and Sommers [8]. The structure was divided into 49 layers of unequal size as indicated by the potential profile in Fig. 6. In Fig. 6 we also show the calculated position of the energy levels in the VSSEF structure for three different applied electric fields. As can be seen from this figure the energy levels in the two smaller quantum wells will align with the second energy level of the 110 Å wide quantum well at a field strength of about 55.5 kV/cm. Fig. 7 present plots of the intensity of the wave functions for the two energy levels $E_2^I = 90.5$ meV and $E^{III} = 91.6$ meV, at a field strength of $\mathfrak{F} = 55.5$ kV/cm. As can be seen in the figure the wave functions are not fully confined to the quantum wells but can penetrate the barriers. In

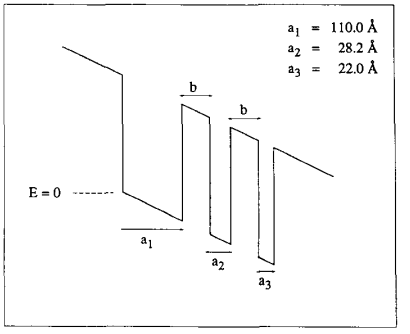

Fig. 5. Schematic representation of the VSSEF-structure. Note the location of the reference level $E = 0$.

Table VIII, we compare our calculated results with those presented by [8]. Energy levels are expressed according to the reference level ($E = 0$) in the lower left corner of the 110 Å wide quantum well (see Fig. 5). The discrepancy of about 10–15 meV between our results and those of [8] is not fully understood. In [8] a well depth of 500 meV was assumed. Changing the well depth from 477 to 500 meV in our calculations results in a shift in the location of the energy levels of only 5 meV. The remaining difference between our results and those of [8] may be due to the use of different effective masses.

IV. DISCUSSION

We have compared our TMM program with results from several other methods. In all these cases, no significant differences appear in the location of the energy levels or wave functions. We conclude that it is much more important to use the appropriate parameters for the effective mass and the band-splitting ratio than to use the most numerically accurate algorithm. The advantage with the transfer matrix method has clearly been shown. The algorithm is easy to implement. The program gives fast and accurate answers and it is applicable to almost any type of one-dimensional problems. We have shown that it is easy to take the variation of the effective mass into account and to calculate energy levels for potential profiles with an applied static electric field.

It may be argued that, in numerical terms, the matrix coefficient α_{22} will never be exactly zero, but just close to zero. Explicitly writing out (4) for the case where $x > x_{N-2}$, we have if $V_{N-1} > E$

$$\Psi_{N-1}(x) = \alpha_{12} \cdot B_0 \cdot e^{-b \cdot (x - x_{N-1})} + \alpha_{22} \cdot B_0 \cdot e^{b \cdot (x - x_{N-1})} \tag{20}$$

where

$$b = \sqrt{\frac{8\pi^2 \cdot m^*_{N-1}}{h^2} \cdot (V_{N-1} - E)}. \tag{21}$$

As can be seen from (20), the approximation of the wave function will only be accurate in a relatively small range along the x axis where $x > x_{N-1}$, since $\alpha_{22} \neq 0$. The range where the value of $|\Psi|^2$ is correct can be extended by improving the search algorithm and ensure that the cal-

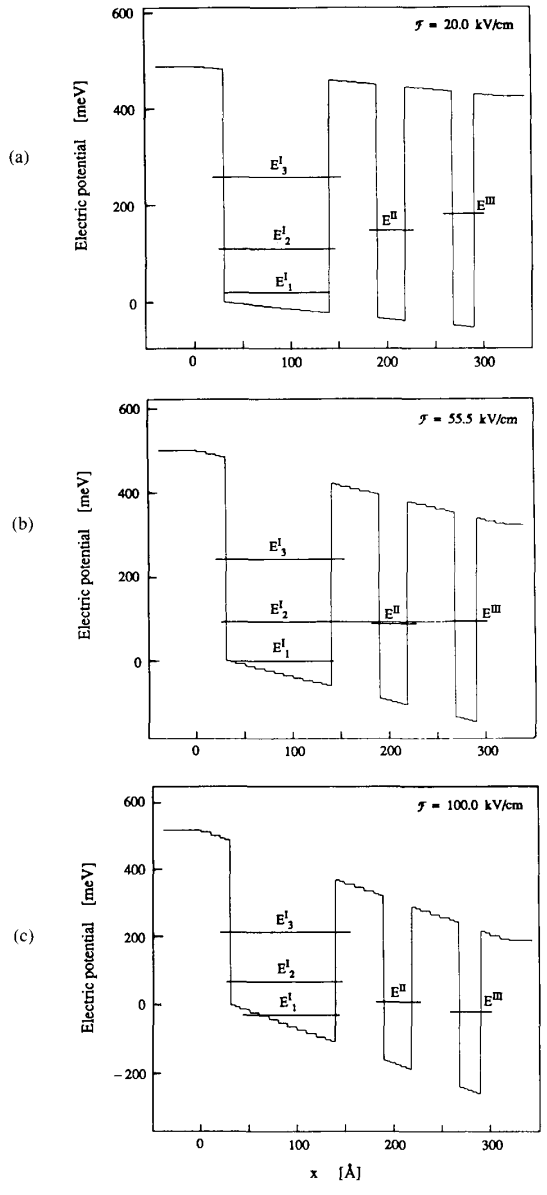

Fig. 6. The location of the energy levels for electrons in the VSSEF structure described in column H of Table I and Fig. 5. The barrier width is b = 50 Å and the applied field is a) 20 kV/cm; b) 55.5 kV/cm; and c) 100 kV/cm.

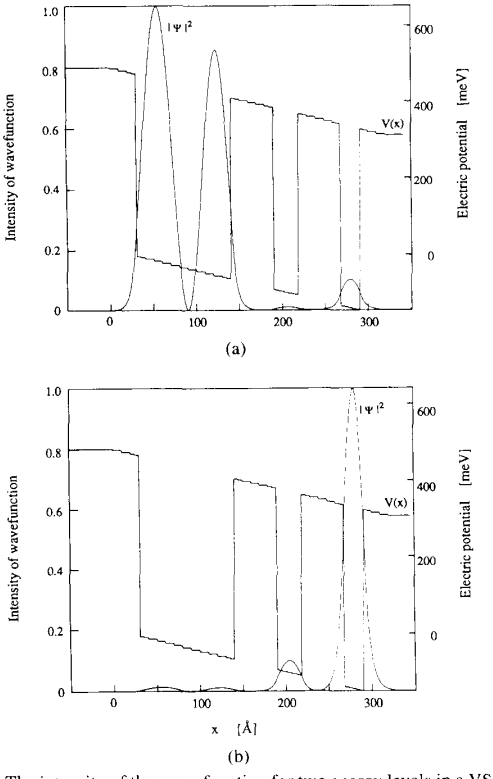

Fig. 7. The intensity of the wave function for two energy levels in a VSSEF structure at an applied field of 55.5 kV/cm. a) $E = E_2^1 = 90.5$ meV b) $E = E^{III} = 91.6$ meV.

culated value of the matrix coefficient α_{22} is smaller than some given value. However, this problem with the shape of the wave function is easily avoided, since in all the examples we have studied, no author has plotted the wave function in a range that exceeds ours, and hence, our method is working just as well as any other.

When searching for quasi-bound states there is a difficulty in finding the correct complex energy levels. For bound states the energy levels are located along the real axis, but for quasi-bound states the energy levels must be expressed as complex numbers. For all practical potential profiles the corresponding imaginary part of the energy levels E_{im} is only a small fraction of the magnitude of the real part E_{re}. In Table VI, for example, E_{im} is in the order of 10^{-2} to 10^{-5} times smaller than E_{re}. Therefore, the search algorithm we use is designed for first making a preliminary search along the real axis. When a rought estimate of E is found, the program continues to refine this value by searching in the complex plane around this preliminary value. There is no difference in the used search-methods depending on whether the energy-values are expected to be bound or quasi-bound. For both cases we execute exactly the same search algorithm. For potential profiles that results in bound states, E_{im} is found to be identically zero. For potential profiles that gives quasi-bound states the calculated value of E_{im} will be not identically zero, but close to zero, as indicated in Table VI. However, this search method only gives accurate results of E_{im} as long as the location of the root is not to far from the real axis. For large electric fields the program might fail to find a correct complex energy level. This effect can be seen when comparing the calculated lifetimes in Table VII. For applied fields from zero to 300 kV/cm the calculated lifetimes do decrease with increasing field strength, but for the calculation at 350 kV/cm the TMM predicts a larger lifetime than for 300 kV/cm.

When comparing our TMM program with sine and cosine wave functions and the Airy-function method [(12)] we found no significant differences between the calculated values. The implementation of routines for calculating Airy-functions is, however, a tedious task. Even though the number of layers decrease when using the Airy-func-

TABLE VIII
CALCULATED ENERGY LEVELS FOR DIFFERENT ELECTRIC FIELDS FOR THE VSSEF STRUCTURE DESCRIBED IN COLUMN H OF TABLE I. OUR RESULTS (TMM) ARE COMPARED TO THOSE OF BRENNAN AND SOMMERS [8] FOR TWO DIFFERENT VALUES OF THE BARRIER WIDTH b. ENERGY LEVELS ARE RELATED TO THE REFERENCE LEVEL $E = 0$, IN FIG. 5.

Applied field		Energy Levels, [meV]			
[kV/cm]	Energy Level No.	TMM	[8]	TMM	[8]
		b = 35 Å		b = 50 Å	
0	E^{I}_{1}	29.8	–	29.7	–
	E^{I}_{2}	119.1	–	119.0	–
	E^{I}_{3}	266.0	–	266.3	–
	E^{II}	181.4	–	180.9	–
	E^{III}	228.2	–	229.2	–
20	E^{I}_{1}	19.0	–	19.0	–
	E^{I}_{2}	108.7	–	108.6	–
	E^{I}_{3}	255.5	–	255.8	–
	E^{II}	147.0	–	149.4	–
	E^{III}	178.9	–	186.1	–
55.5	E^{I}_{1}	– 1.5	–	– 1.5	–
	E^{I}_{2}	90.5	104	93.8	–
	E^{I}_{3}	236.9	242	236.4	–
	E^{II}	85.5	98	89	–
	E^{III}	91.6	109.5	110.4	–
66.6	E^{I}_{1}	– 8.3	–	– 8.3	–
	E^{I}_{2}	84.8	–	84.5	93
	E^{I}_{3}	231.1	–	231.4	239
	E^{II}	62.9	–	73.0	80
	E^{III}	67.6	–	88	110
100	E^{I}_{1}	– 29.3	–	– 29.3	–
	E^{I}_{2}	68.2	–	68.5	–
	E^{I}_{3}	213.9	–	214.3	–
	E^{II}	9.6	–	27.1	–
	E^{III}	– 19.0	–	8.9	–

tion algorithm the numerical errors might increase if the Airy-functions are not evaluated properly. The advantage of these Airy-function solutions is that, when working with linearly varying potentials, there is no need to divide the potential profile into several small layers. Thus the numerical errors due to approximations in each layer will decrease. On the other hand, there is a problem in calculating the Airy-functions correctly. This is especially difficult if the slope of the potential profile is close to zero. The conclusion is that the transfer matrix method with sine and cosine wave functions [(4)] in general is more reliable and gives just as accurate results as the Airy-function method.

V. CONCLUSION

A fast and accurate algorithm for solving the one-dimensional time-independent Schrödinger equation for a piecewise-constant potential profile has been presented and compared to other methods. Since any potential profile can be approximated to arbitrary accuracy using a piecewise constant function, the Schrödinger equation can, in principle, be solved for any potential profile. We have showed that this method can easily be used for a large variety of problems. The transfer matrix method involves straightforward multiplication of 2×2 matrices and is simple to implement on a computer. The method presented here gives not only the correct complex eigenvalues (energy levels), but also the correct wave functions which makes it a very valuable tool when analyzing quantum-well structures.

We have compared our implemented transfer matrix method with results from several other methods, including the more complex finite element method. The energy values, calculated with the TMM, are correct to an accuracy of at least three digits. In cases where we have had discrepancies between our results and those of others it has been due to the fact that we have used different input parameters, such as the effective masses and the band-splitting parameter. We show that the use of correct values of m^* and Q_c, although often neglected, is far more important than the numerical accuracy of the algorithm.

VI. Acknowledgment

The authors would like to thank Dr. P. Andersson and Dr. P. Andrekson for their helpful suggestions and careful examination of this paper.

References

[1] W. T. Tsang, "Molecular beam epitaxy for III-V compound semiconductors," in *Semiconductors and Semimetals*, W. T. Tsang, Ed. New York: Academic, 1985, vol. 22, Part A, pp. 95-208, ch. 2.

[2] G. B. Stringfellow, "Organometallic vapor-phase epitaxial growth of III-V semiconductors," in *Semiconductors and Semimetals*, W. T. Tsang, Ed. New York: Academic, 1985, vol. 22, Part A, ch. 3, pp. 209-255.

[3] A. C. Gossard, "Growth of microstructures by molecular beam epitaxy," *IEEE J. Quantum Electron.*, vol. QE-22, no. 9, pp. 1649-1655, Sept. 1986.

[4] L. Esaki, "A bird's-eye view on the evolution of semiconductor superlattices and quantum wells," *IEEE J. Quantum Electron.*, vol. QE-22, no. 9, pp. 1611-1624, Sept. 1986.

[5] L. M. Walpita, "Solutions for optical waveguide equations by selecting zero elements in a characteristic matrix," *J. Opt. Soc. Amer. A*, vol. 2, no. 4, pp. 595-602, Apr. 1985.

[6] A. K. Ghatak, K. Thyagarajan, and M. R. Shenoy, "Numerical analysis of planar optical waveguides using matrix approach," *J. Lightwave Technol.*, vol. LT-5, no. 5, pp. 660-667, May 1987.

[7] T. Makino and J. Glinski, "Transfer matrix analysis of the amplified spontaneous emission of DFB semiconductor laser amplifiers," *IEEE J. Quantum Electron.*, vol. 24, no. 8, pp. 1507-1518, Aug. 1988.

[8] K. E. Brennan and C. J. Summers, "Theory of resonant tunneling in a variably spaced multiquantum well structure: An Airy-function approach," *J. Appl. Phys.*, vol. 61, no. 2, pp. 614-623, Jan. 1987.

[9] E. Merzbacher, *Quantum Mechanics*, 2nd ed. New York: Wiley, 1970, ch. 7.

[10] G. Bastard, E. E. Mendez, L. L. Chang, and L. Esaki, "Variational calculations on a quantum well in an electric field," *Phys. Rev. B*, vol. 28, no. 6, pp. 3241-3245, Sept. 1983.

[11] D. Ahn and S. L. Chuang, "Variational calculations of subbands in a quantum well with uniform electric field: Gram-Schmidt ortogonalization approach," *Appl. Phys. Lett.*, vol. 49, no. 21, pp. 1450-1452, Nov. 1986.

[12] A. K. Ghatak, K. Thyagarajan, and M. R. Shenoy, "A novel numerical technique for solving the one-dimensional Schrödinger equation using matrix approach—Application to quantum-well structures," *IEEE J. Quantum Electron.*, vol. 24, no. 8, pp. 1524-1531, Aug. 1988.

[13] F. Borondo and J. Sánchez-Dehesa, "Electronic structure of a GaAs quantum well in an electric field," *Phys. Rev. B*, vol. 33, no. 12, pp. 8758-8761, June 1986.

[14] J. Singh, "A new method for solving the ground-state problem in arbitrary quantum wells: Application to electron-hole quasi-bound levels in quantum wells under high electric field," *Appl. Phys. Lett.*, vol. 48, no. 6, pp. 434-436, Feb. 1986.

[15] K. Hayata, M. Koshiba, K. Nakamura, and A. Shimizu, "Eigenstate calculations of quantum well structures using finite elements," *Electron. Lett.*, vol. 24, no. 10, pp. 614-616, May 1988.

[16] K. Nakamura, A. Shimizu, M. Koshiba, and K. Hayata, "Finite element analysis of quantum wells of arbitrary semiconductors with arbitrary potential profiles," *IEEE J. Quantum Electron.*, vol. 25, no. 5, pp. 889-895, May 1989.

[17] G. Bastard, "Superlattice band structure in the envelope-function approximation," *Phys. Rev. B*, vol. 24, no. 10, pp. 5693-5697, Nov. 1981.

[18] G. Bastard and J. A. Brum, "Electronic states in semiconductor heterostructures," *IEEE J. Quantum Electron.*, vol. QE-22, no. 9, pp. 1625-1644, Sept. 1986.

[19] B. Jonsson and S. T. Eng, "Solving the one-dimensional time-independent Schrödinger equation by the transfer matrix method: Applications to quantum well structures," Dept. of Optoelectron. and Elec. Meas., Chalmers University of Technology, Sweden, 1989, Tech. Rep. No. TR 89237.

[20] E. J. Austin and M. Jaros, "Electronic structure of an isolated GaAs-GaAlAs quantum well in a strong electric field," *Phys. Rev. B*, vol. 31, no. 8, pp. 5569-5572, Apr. 1985.

[21] D. Ahn and S. L. Chuang, "Exact calculations of quasibound states of an isolated quantum well with uniform electric field: Quantum well stark resonance," *Phys. Rev. B*, vol. 34, no. 12, pp. 9034-9037, Dec. 1986.

[22] W. W. Lui and M. Fukuma, "Exact solution of the Schrödinger equation across an arbitary one-dimensional piecewise-linear potential barrier," *J. Appl. Phys.*, vol. 60, no. 5, pp. 1555-1559, Sept. 1986.

[23] S. Adachi, "GaAs, AlAs, and $Al_xGa_{1-x}As$: Material parameters for use in research and device applications," *J. Appl. Phys.*, vol. 58, no. 3, pp. R1-R29, Aug. 1985.

[24] K. Bajema, R. Merlin, F. Y. Juang, S. C. Hong, J. Singh, and P. K. Bhattacharya, "Stark effect in GaAs-$Al_xGa_{1-x}As$ quantum wells: Light scattering by intersubband transitions," *Phys. Rev. B*, vol. 36, no. 2, pp. 1300-1302, July 1987.

[25] D. A. B. Miller, D. S. Chemla, T. C. Damen, A. C. Gossard, W. Wiegmann, T. H. Wood, and C. A. Burrus, "Electric field dependence of optical absorption near the band gap of quantum-well structures," *Phys. Rev. B*, vol. 32, no. 2, pp. 1043-1060, July 1985.

Björn M. Jonsson (S'86) was born in Stockholm, Sweden, on August 28, 1960. He received the M.Sc. degree in engineering physics from Chalmers University of Technology, Göteborg, Sweden in 1986.

In 1986 he joined the Research Laboratory at the Department of Optoelectronics and Electrical Measurements, Chalmers University of Technology, where he is currently pursuing the Ph.D. degree. His current research interests are in numerical modeling of optoelectronic devices.

Sverre T. Eng (M'58) received the M.S. degree in electrical engineering in 1953 and the Ph.D. degree in applied physics in 1967, both from Chalmers University of Technology, Göteborg, Sweden.

From 1953 to 1956 he was engaged in the research and development of ultrasensitive microwave receivers for radio astronomy at Chalmers University of Technology. He later (1956-1967) spent ten years at Hughes Research Laboratories, Newport Beach, CA, as a member of the Technical Staff, as Section Head and Department Head, where he built up a research department in microwave and optical solid-state electronics. He initiated research on parametric diodes, mixers, tunnel diodes, optical detectors, semiconductor lasers, and instrumentation. In 1967 he joined North American Rockwell Corporation, Anaheim, CA, and spent four years conducting research on lasers and electrooptic systems. Since 1971, he has been Professor and Director of the Department of Optoelectronics and Electrical Measurements, Chalmers University of Technology, where he has conducted research on fiber-optics communication, applied laser spectroscopy, and optical and digital computers in scientific instrumentation. On leave from Chalmers University of Technology, he has worked as a consultant and Division Technologist at the Jet Propulsion Laboratory, California Institute of Technology, Pasadena, in the areas of long-range R&D planning, fiber optics, integrated optics, and optical information processing research. He is the author of more than 100 technical publications and has several patents.

Dr. Eng is a member of the Royal Swedish Academy of Engineering Sciences, American Physical Society, and the Optical Society of America.